NASA Contractor Report 172261

Skin/Stiffener Interface Stresses in Composite Stiffened Panels

J. T. S. Wang
S. B. Biggers

LOCKHEED-GEORGIA COMPANY
A Division of Lockheed Corporation
Marietta, Georgia

Contract NAS1-15949
January 1984

National Aeronautics and
Space Administration

Langley Research Center
Hampton, Virginia 23665

FOREWORD

This report is prepared by the Lockheed-Georgia Company under contract NAS1-15949, "Advanced Composite Structural Design Technology for Commercial Transport Aircraft." It describes in detail an analysis procedure for determining the stresses in the interface layer between the skin and attached flange of stiffened composite panels. This work was performed under Task Assignment No. 5 of the contract. The program is sponsored by the National Aeronautics and Space Administration, Langley Research Center (NASA/LaRC). Dr. James H. Starnes is the Project Engineer for NASA/LaRC. John N. Dickson is the Program Manager for the Lockheed-Georgia Company. J.T.S. Wang, Professor in the School of Engineering Science and Mechanics at Georgia Institute of Technology, is a consultant to Lockheed-Georgia.

TABLE OF CONTENTS

SUMMARY

A structural model and an analysis method for evaluating the stresses in the interface layer between the skin and the attached stiffener flange of stiffened composite panels is described. When stiffened panels are loaded in the postbuckling regime and/or are subject to normal pressure loads, deformations develop that tend to cause separation of the skin and the stiffeners. The analysis procedure described here provides a means to study the effects of material and geometric design parameters on the interface stresses. The tendancy toward skin/stiffener separation may therefore be minimized by chosing appropriate values for the design variables. This interface stress analysis procedure is included in a stiffened panel sizing code previously developed and reported under this contract (References 1 and 2).

INTRODUCTION

Panels stiffened with attached stiffeners are frequently used in aerospace, naval, and various civil engineering structures when structural weight is an important concern. If the panel is loaded so that the skin (web) enters the postbuckling regime and/or the panel is subject to normal pressure loads, the skin and stiffener tend to separate. Postbuckling deformation is shown in Figure 1. Separation of the skin and stiffener normally indicates or participates in failure of the panel.

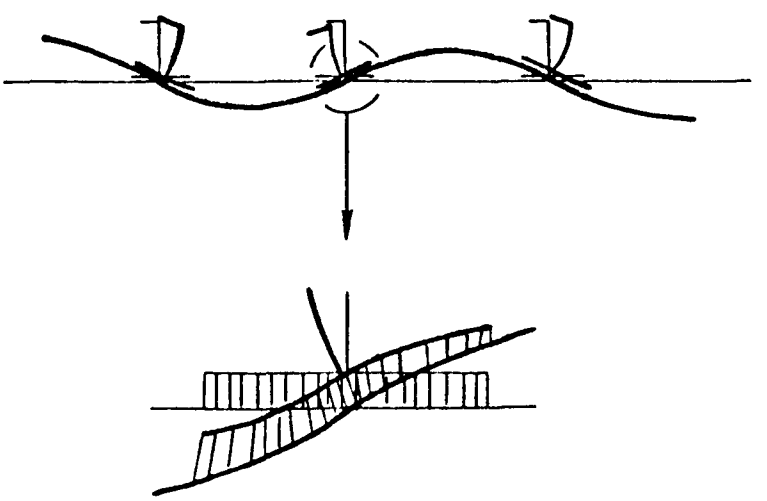

Figure 1. Deformation of Postbuckled Stiffened Panel

Resin-matrix composite stiffened panels are normally fabricated by cocuring the skin and stiffeners or by bonding precured stiffeners to the skin. Mechanical fasteners or stitching may also be used to attach the stiffeners to the skin in some cases.

The purpose of this study is to develop a model and solution method for determining the normal and shear stresses in the interface between the skin and the stiffener attached flange. An efficient, analytical solution procedure is required since the analysis is incorporated in a sizing code for stiffened panels (References 1 and 2). The present model does not account for the presence of mechanical fasteners or stitching.

STRUCTURAL MODEL

The portion of the stiffened panel that is modeled includes the attached flange of the stiffener, the skin directly in contact with the stiffener, and the interface or bond layer. The model is shown in Figure 2. The skin between stiffeners is replaced by moments and shear loads obtained from an independent solution for the response of the skin plate to the applied panel loads. The deformation of the skin between stiffeners may not be small enough, especially if the skin is postbuckled, to allow small deformation theory to be used. It is assumed, however, that the deformations of the stiffener flange and the attached portion of the skin are small and that small deformation theory is valid for this region of the panel.

The stiffener web is replaced by rotational and extensional springs along the line $y = z = 0$ with stiffnesses k_r and k_z, respectively. A longitudinal inplane load, N_x^f, is present in the stiffener flange and biaxial inplane loads, N_x and N_y, are present in the skin. A transverse extensional spring, representing the transverse stiffness (k_y) of the skin, is present on the edges $y = \pm b$ of the skin plate. Both flange and skin plates are orthotropic.

The interface layer between the flange and skin has a finite thickness, t_a, and is assumed to be isotropic and linear elastic. Stresses in the interface layer are distributed uniformly through the thickness of the layer.

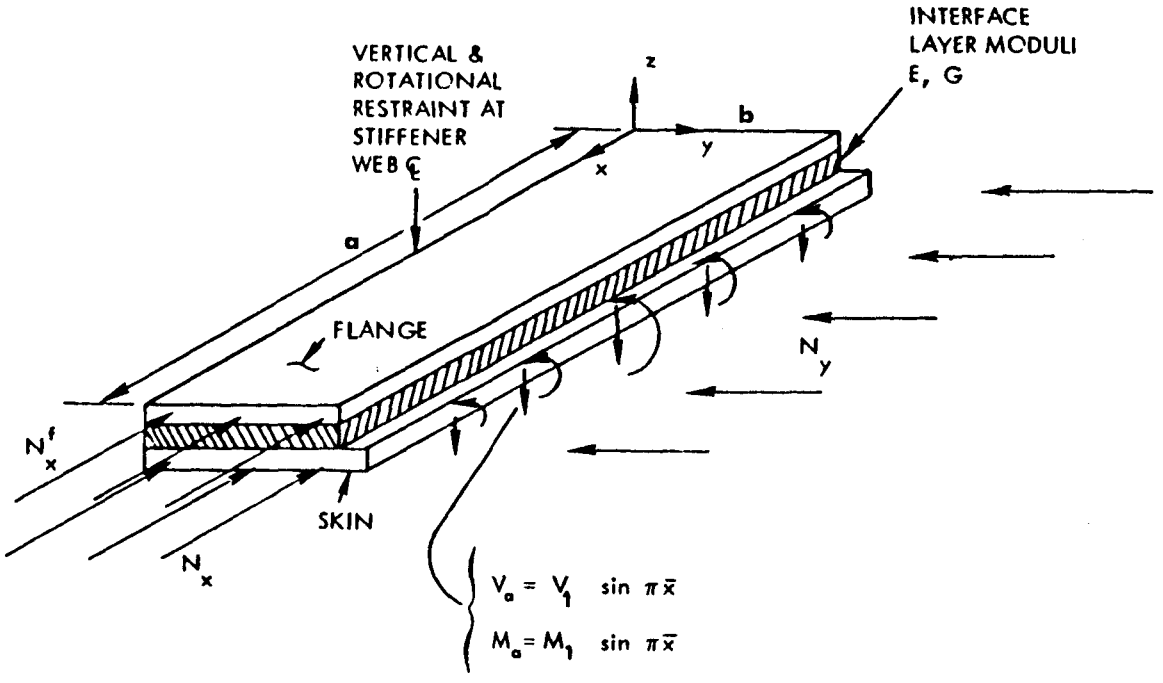

Figure 2. Structural Model for Interface Stress Analysis

ANALYSIS METHOD

The flange and skin plates are treated as separate orthotropic plates. The plates are loaded on the interface planes by the unknown interface normal and shear stresses and on the longitudinal skin plate edges by the applied moment and transverse shear loads due to normal pressure and/or postbuckling. The inplane loads previously defined are assumed to remain unchanged during deformation.

The displacements of the plates in the x, y, and z directions are u, v, and w, respectively. Using a comma followed by a subscript to denote differentiation, the relations of stress resultants and stress couples to the displacements and interacting interface stresses may be expressed as follows:

$$N_{xx} = A_{11}\, u_{,x} + A_{12}\, v_{,y} \tag{1}$$

$$N_{yy} = A_{21}\, u_{,x} + A_{22}\, v_{,y} \tag{2}$$

$$N_{xy} = A_{66}\, (u_{,y} + v_{,x}) \tag{3}$$

$$M_{xx} = -D_{11}\, w_{,xx} - D_{12}\, w_{,xy} \tag{4}$$

$$M_{yy} = -D_{21}\, w_{,xx} - D_{22}\, w_{,yy} \tag{5}$$

$$M_{xy} = -2D_{66}\, w_{,xy} \tag{6}$$

$$Q_x = -D_{11}\, w_{,xxx} - (D_{12} + 2D_{66})\, w_{,xyy} + (t/2)(\tau_{xz}^{+} - \tau_{xz}^{-}) \tag{7}$$

$$Q_y = -(D_{12} + 2\, D_{66})\, w_{,xxy} - D_{22}\, w_{,yyy} + (t/2)(\tau_{yz}^{+} - \tau_{yz}^{-}) \tag{8}$$

$$V_x = Q_x + M_{xy,y} \tag{9}$$

$$V_y = Q_y + M_{yx,x} \tag{10}$$

in which the A_{ij} are the inplane stiffnesses, the D_{ij} are the bending stiffnesses, the tangential loading components on the upper and lower surfaces of the plate are τ_{xz}^{+}, τ_{yz}^{+} and τ_{xz}^{-}, τ_{yz}^{-} respectively, and t is the plate thickness. The tangential loadings are zero on the plate free surfaces and represent the interface shear stresses on the interface surfaces. The normal surface loading on the plates is denoted σ_z^{+}, σ_z^{-} and represents the interface normal stress.

The general equations for the analysis of the skin and the flange plates may be obtained as follows. For a plate in a region A, with the boundary S, and having lines of elastic support S_j, the principle of virtual work may be expressed as

$$\delta\pi = \iint_A [N_{\alpha\beta}\, \delta\varepsilon_{\alpha\beta} - M_{\alpha\beta}\, (\delta w)_{,\alpha\beta} - (\tau_{z\alpha}^{+} - \tau_{z\alpha}^{-})\, \delta U_\alpha - (\sigma_z^{+} - \sigma_z^{-})\, \delta w]\, dx\, dy$$

$$- \oint_S [N_{nna}\, \delta U_n + N_{nsa}\, \delta U_s + M_{nna}\, (\delta w)_{,n} + V_{na}\, \delta w]\, ds$$

$$- \sum_j \oint_{S_j} [k_n U_n\, \delta U_n + k_s U_s\, \delta U_s + k_z w\, \delta w + k_r w_{,n}\, (\delta w)_{,n}]\, ds_j = 0 \tag{11}$$

where π is the total potential energy, and n and s refer respectively to the outward normal and tangential directions along the plate boundaries or lines of elastic support. The subscript "a" denotes shear, moment, and inplane loads applied along the edge of the plate. The usual index notation is

followed for α and β ranging from 1 to 2 with 1 corresponding to α and 2 to y. The inplane displacements U_n and U_s are related to U_α. The stiffnesses of elastic supports are k_n, k_s, k_z and k_r. To account for the effects of inplane loading, the inplane strain-displacement relations $\epsilon_{\alpha\beta} = (U_{\alpha,\beta} + U_{\beta,\alpha} + w_{,\alpha} w_{,\beta})/2$ are used and the relations $Q_\alpha = M_{\beta\alpha,\beta}$ are recognized in equation (11). After employing Green's theorem, equation (11) may be written as

$$\begin{aligned}
\delta\pi = & -\iint_A \{[N_{\beta\alpha,\beta} + (\tau^+_{z\alpha} - \tau^-_{z\alpha})]\,\delta U_\alpha \\
& + [M_{\alpha\beta,\alpha\beta} + (N_{\alpha\beta} w_{,\alpha})_{,\beta} + (\sigma^+_z - \sigma^-_z)\,\delta w\}\,dx\,dy \\
& + \oint_S [(N_{nn} - N_{nna})\,\delta U_n + (N_{ns} - N_{nsa})\,\delta U_s \\
& + (M_{nn} - M_{nna})(\delta w)_{,n} + (V_n + N_{nna} w_{,n} + N_{nsa} w_{,s} - V_{na})\,\delta w]\,ds \\
& - \sum_j \int_{S_j} [k_n U_n\,\delta U_n + k_s U_s\,\delta U_s + k_z w\,\delta w + k_r w_{,n}(\delta w)_{,n}]\,ds_j = 0
\end{aligned} \tag{12}$$

In equation (12), we require integrals involving the variations of U_α and w to vanish individually. This results in three equations in integral form. The inplane stress resultants, $N_{11} = -N_x$, $N_{22} = -N_y$ and $N_{12} = 0$, are assumed to be distributed uniformly prior to the bending of the plate. The U_α represent incremental inplane displacements after bending. Using dimensionless coordinates defined as $\bar{x} = x/a$ and $\bar{y} = y/b$, the aspect ratio $r = a/b$, the half-plate thickness, $e = t/2$, and an over dot and over prime for differentiation with respect to $\bar{x}$ and $\bar{y}$, respectively, the three equations with linearized coefficients may be written as follows:

$$\begin{aligned}
& \int_0^1 \int_{-1}^1 [A_{11}\,\ddot{u}/r^2 + A_{66}\,u'' + (A_{12} + A_{66})\,\dot{v}'/r + b^2(\tau^+_{xz} - \tau^-_{xz})]\,\delta u\,d\bar{x}\,d\bar{y} \\
& + (1/r) \int_{-1}^1 [(bN_x - A_{11}\,\dot{u}/r - A_{12}\,\dot{v})\ \delta u]_{\bar{x}=1}\,d\bar{y} \\
& -(1/r) \int_{-1}^1 [(bN_x - A_{11}\,\dot{u}/r - A_{12}\,v')\ \delta u]_{\bar{x}=0}\,d\bar{y} \\
& - \int_0^1 [A_{66}(u' + \dot{v}/r)\ \delta u]_{\bar{y}=1}\,d\bar{x} + \int_0^1 [A_{66}(u' + \dot{v}/r)\,\delta u]_{\bar{y}=-1}\,d\bar{x} = 0
\end{aligned} \tag{13}$$

$$\int_0^1 \int_{-1}^1 [A_{22}\, \ddot{v}'' + A_{66}\, \ddot{v}/r^2 + (A_{12} + A_{66})\, \dot{u}'/r + b^2\, (\tau_{yz}^+ - \tau_{yz}^-)]\, \delta v\, d\bar{x}d\bar{y}$$

$$+ \int_0^1 [(bN_y - A_{22}\, \dot{v}' - A_{21}\, \dot{u}/r)\, \delta v]_{\bar{y}=1}\, d\bar{x}$$

$$- \int_0^1 [(bN_y - A_{22}\, \dot{v}' - A_{21}\, \dot{u}/r)\, \delta v]_{\bar{y}=1}\, d\bar{x}$$

$$+ (1/r) \int_{-1}^1 [(A_{66}\, (\dot{u}' + \dot{v}'/r)\, \delta v]_{\bar{x}=0}\, d\bar{y} - (1/r) \int_{-1}^1 [A_{66}\, (\dot{u}' + \dot{v}'/r)\, \delta v]_{\bar{x}=1}\, d\bar{y}$$

$$+ b \int_0^1 (k_y\, v\, \delta v)_{\bar{y}=1}\, d\bar{x} + b \int_0^1 (k_y\, v\, \delta v)_{\bar{y}=-1}\, d\bar{x} = 0 \qquad (14)$$

$$\int_0^1 \int_{-1}^1 [D_{11}\, \ddot{w}''/r^4 + 2(D_{12} + 2D_{66})\, \ddot{w}''/r^2 + D_{22}\, w'''' + (\sigma_z^- - \sigma_z^+)\, b^4$$

$$+ N_x\, b^2\, \ddot{w}/r^2 + N_y\, b^2\, w'' - eb^3\, (\dot{\tau}_{xz}^+/r - \dot{\tau}_{xz}^-/r + \tau_{yz}^{+\prime} - \tau_{yz}^{-\prime})]\, \delta w\, d\bar{x}d\bar{y}$$

$$- \int_0^1 [(M_{ya}\, b^2 + D_{22}\, w'' + D_{21}\, \ddot{w}/r^2)\, \delta \dot{w}]_{\bar{y}=-1}\, d\bar{x}$$

$$+ \int_0^1 [(M_{ya}\, b^2 + D_{22}\, w'' + D_{21}\, \ddot{w}/r^2)\, \delta \dot{w}]_{\bar{y}=1}\, d\bar{x}$$

$$+ \int_0^1 \{[V_{ya} b^3 + N_y\, b^2\, \dot{w}' + D_{22}\, w''' + (D_{12} + 4D_{66})\, \ddot{w}''/r^2 - eb^3\, (\tau_{yz}^+ - \tau_{yz}^-)]\, \delta w\}_{\bar{y}=-1}\, d\bar{x}$$

$$- \int_0^1 \{[V_{ya} b^3 + N_y\, b^2\, \dot{w}' + D_{22}\, w''' + (D_{12} + 4D_{66})\, \ddot{w}''/r^2 - eb^3\, (\tau_{yz}^+ - \tau_{yz}^-)]\, \delta w\}_{\bar{y}=1}\, d\bar{x}$$

$$+ \int_{-1}^1 \{(b/r)^2\, [M_{xa} + D_{11}\, \ddot{w}/r^2 + D_{12}\, w'']\, \delta \dot{w}\}_{\bar{x}=1}\, d\bar{y}$$

$$- \int_{-1}^1 \{(b/r)^2\, [M_{xa} + D_{11}\, \ddot{w}/r^2 + D_{12}\, w'']\, \delta \dot{w}\}_{\bar{x}=0}\, d\bar{y}$$

$$- \int_{-1}^1 \{(1/r)\, [b^3\, V_{xa} + b^2\, N_x\, \dot{w}/r + D_{11}\, \dddot{w}/r^3 + (D_{12} + 4D_{66})\, \ddot{w}''/r$$

$$-eb^3\, (\tau_{xz}^+ - \tau_{xz}^-)]\, \delta w\}_{\bar{x}=1}\, d\bar{y}$$

$$+ \int_{-1}^1 \{(1/r)\, [b^3\, V_{xa} + b^2\, N_x\, \dot{w}/r + D_{11}\, \dddot{w}/r^3 + (D_{12} + 4D_{66})\, \ddot{w}''/r$$

$$-eb^3\, (\tau_{xz}^+ - \tau_{xz}^-)]\, \delta w\}_{\bar{x}=0}\, d\bar{y} + b \int_0^1 (k_z\, w\, \delta w + k_r\, \dot{w}\, \delta \dot{w})_{\bar{y}=0}\, d\bar{x} = 0 \qquad (15)$$

where the subscript "a" denotes applied longitudinal edge shear and moment loads. Equations (13) - (15) may be written for the flange plate and the skin plate.

Solutions for the response of the plates and the resulting interface stresses may be developed separately for the antisymmetric and the symmetric load cases.

ANTISYMMETRIC DEFORMATION

If the web of the stiffener is along the center line of the flange and the stiffened panel is postbuckled but is subject to no normal pressure load, the flange and skin plates will deform antisymmetrically about y = 0. The applied longitudinal edge loads are

$$M_a|_{\bar{y}=1} = -M_a|_{\bar{y}=-1} = M(\bar{x}) \tag{16}$$

$$V_a|_{\bar{y}=1} = V_a|_{\bar{y}=-1} = V(\bar{x}) \tag{17}$$

The displacements and interface stresses are represented in the following series form with n = 0, 2, 4 . . . ; m = 0, 1, 2, 3 . . . ; and

$$M(\bar{x}) = \sum_m M_m \sin m\pi\bar{x} \tag{18}$$

$$V(\bar{x}) = \sum_m V_m \sin m\pi\bar{x} \tag{19}$$

$$u = \sum_m \sum_n U_{mn} P_{n+1}(\bar{y}) \cos m\pi\bar{x} \tag{20}$$

$$v = \sum_m \sum_n V_{mn} P_n(\bar{y}) \sin m\pi\bar{x} \tag{21}$$

$$w = \sum_m \sum_n W_{mn} P_{n+1}(\bar{y}) \sin m\pi\bar{x} \tag{22}$$

$$p_x = \sum_m \sum_n p_{xmn} P_{n+1}(\bar{y}) \cos m\pi\bar{x} \tag{23}$$

$$p_y = \sum_m \sum_n p_{ymn} P_n(\bar{y}) \sin m\pi\bar{x} \tag{24}$$

$$q = \sum_m \sum_n q_{mn} P_{n+1}(\bar{y}) \sin m\pi\bar{x} \tag{25}$$

where the $P_n(y)$ are Legendre polynomials.

The nonzero surface loads on the skin plate are

$$\tau_{xz}^{+} = p_x \qquad \tau_{yz}^{+} = p_y \qquad \sigma_z^{+} = q \tag{26}$$

The nonzero surface loads on the flange plate are

$$\tau_{xz}^{-} = p_x \qquad \tau_{yz}^{-} = p_y \qquad \sigma_z^{-} = q \tag{27}$$

Substitution of equations (20), (21), (23), and (24) into equations (13), and (14) written for the skin plate yields

$$\begin{bmatrix} [a_m] & [b_m] \\ [c_m] & [d_m] \end{bmatrix} \begin{Bmatrix} \{U_m\} \\ \{V_m\} \end{Bmatrix} = \begin{bmatrix} [g_m] & [o] \\ [o] & [k_m] \end{bmatrix} \begin{Bmatrix} \{p_{xm}\} \\ \{p_{ym}\} \end{Bmatrix} \tag{28}$$

in which for $j \geq n$ the elements of the matrices are

$$a_{mjn} = \bar{m}^2 A_{11} \delta_{jn}/(2n+3) + A_{66} P_{j+1}(1) P'_{n+1}(1) \tag{29}$$

$$b_{mjn} = \bar{m} A_{66} P_{j+1}(1) P_n(1) \tag{30}$$

$$c_{mjn} = \bar{m} [(A_{12} + A_{66}) \delta_{jn} - A_{21} P_j(1) P_{n+1}(1) \tag{31}$$

$$d_{mjn} = A_{22} P_j(1) P'_n(1) + \bar{m}^2 A_{66} \delta_{jn}/(2n+1) + k_y P_n(1) P_j(1) \tag{32}$$

$$g_{mjk} = b^2 \delta_{jn}/(2n+3) \tag{33}$$

$$k_{mjn} = b^2 \delta_{jn}/(2n+1) \tag{34}$$

where $\bar{m} = m\pi/r$.

Since the coefficient matrix in equation (28) must be symmetric, for each m and for $j \geq n$

$$a_{mnj} = a_{mjn} \qquad b_{mnj} = c_{mjn}$$
$$c_{mnj} = b_{mjn} \qquad d_{mnj} = d_{mjn} \tag{35}$$

Equations (28) may be written for the flange plate if A^f_{ij} are used in equations (29) - (32), k_y is set equal to zero, and the symbols a^f_{mnj}, b^f_{mnj}, c^f_{mnj}, and d^f_{mnj} are used for the flange.

Substitution of equations (22) - (25) into equation (15) written for the flange and for the skin yields

$$[s^f_m]\{p_{xm}\} + [r^f_m]\{p_{ym}\} - [h^f_m]\{q_m\} - [\beta^f_m]\{W^f_m\} = \{0\} \tag{36}$$

$$[s_m]\{p_{xm}\} + [r_m]\{p_{ym}\} + [h_m]\{q_m\} - [\beta_m]\{W_m\} = b^2 M_m \{P'\} - b^3 V_m \{P\} \tag{37}$$

in which, for the skin equation (37), and for $j \geq n$, the elements of the matrices are

$$s_{mjn} = -\bar{m}\, e\, b^3\, \delta_{jn}/(2n+3) \tag{38}$$

$$r_{mjn} = -e\, b^3\, P_{j+1}(1)\, P_n(1) \tag{39}$$

$$h_{mjn} = b^4\, \delta_{jn}/(2n+3) \tag{40}$$

$$\beta_{mjn} = (\bar{m}^{-4} D_{11} - \bar{m}^{-2} b^2 N_x) \delta_{jn}/(2n+3)$$

$$+ P'_{j+1}(1) [D_{22} P''_{n+1}(1) - D_{21} \bar{m}^{-2} P_{n+1}(1)]$$

$$- P_{j+1}(1) [D_{22} P'''_{n+1}(1) - (D_{12} + 4D_{66}) \bar{m}^{-2} P'_{n+1}(1) + N_y b^2 P'_{n+1}(1)]$$

$$+ (k_r/2)b P'_{j+1}(0) P'_{n+1}(0) \tag{41}$$

$$P_j = P_{j+1}(1) \tag{42}$$

$$P'_j = P'_{j+1}(1) \tag{43}$$

The coefficients for the flange equation may be obtained from equations (38) - (41) by using e^f, D_{ij}^f, and N_x^f and setting $N_y = 0$. In normal usage, the rotational restraint (k_r) at y = 0 will be zero on the skin and nonzero on the flange. Equations (28), (36), and (37) relate the displacement coefficients to the interface stress coefficients defined in equations (20) - (25).

The displacements of the skin and flange plates are coupled through the elastic interface layer having thickness h and moduli E and G. The continuity conditions are

$$u^f = u - (e^f + e) w_{,x} + (h/G) p_x - e^f (h/E) q_{,x} \tag{44}$$

$$v^f = v - (e^f + e) w_{,y} + (h/G) p_y - e^f (h/E) q_{,y} \tag{45}$$

$$w^f = w + (h/E) q \tag{46}$$

Substitution of these continuity conditions in conjunction with the series expressions for the displacements and interface stresses, equations (20) - (25), into equations (13) - (14), based on the Galerkin procedure and written for the flange plate, yields the following equations:

$$\left[\left[a_m^f\right]\left[\bar{a}_m\right] + \left[b_m^f\right]\left[\bar{c}_m\right] + (h/G)\left[a_m^f\right] + (1/b)^2\left[h_m\right]\right]\left\{p_{xm}\right\}$$
$$+\left[\left[a_m^f\right]\left[\bar{b}_m\right] + \left[b_m^f\right]\left[\bar{d}_m\right] + (h/G)\left[b_m^f\right]\right]\left\{p_{ym}\right\}$$
$$+\left[\theta_m\right]\left\{q_m\right\} + \left[\varepsilon_m\right]\left\{W_m\right\} = \left\{0\right\} \tag{47}$$

$$\left[\left[c_m^f\right]\left[\bar{a}_m\right] + \left[d_m^f\right]\left[\bar{c}_m\right] + (h/G\left[c_m^f\right]\right]\left\{p_{xm}\right\}$$
$$+\left[\left[c_m^f\right]\left[\bar{b}_m\right] + \left[d_m^f\right]\left[\bar{d}_m\right] + (h/g)\left[d_m^f\right] + (1/b)^2\left[\bar{h}_m\right]\right]\left\{p_{ym}\right\}$$
$$+\left[\bar{\theta}_m\right]\left\{q_m\right\} + \left[\bar{\varepsilon}_m\right]\left\{W_m\right\} = \left\{0\right\} \tag{48}$$

in which, for $j \geq n$, the elements of the matrices are

$$\theta_{mjn} = h\, e^f\, (Z_{mjn} - \bar{m}\, a^f_{mjn})/(bE) \tag{49}$$

$$\varepsilon_{mjn} = -\,(e^f + e)\, E\, \theta_{mjn}/(e^f\, h) \tag{50}$$

$$\bar{\theta}_{mjn} = h\, e^f\, (\bar{Z}_{mjn} - \bar{m}\, c^f_{mjn})/(bE) \tag{51}$$

$$\bar{\varepsilon}_{mjn} = -\,(e^f + e)\, E\, \bar{\theta}_{mjn}/(e^f\, h) \tag{52}$$

$$Z_{mjn} = -\,\bar{m}\, A^f_{66}\, P'_{n+1}(1)\, P_{j+1}(1) \tag{53}$$

$$\bar{Z}_{mjn} = A^f_{22}\, P''_{n+1}(1)\, P_j(1) - \bar{m}^2\, A^f_{66}\ \delta_{nj} \tag{54}$$

and

$$\begin{bmatrix}\left[\bar{a}_m\right] & \left[\bar{b}_m\right] \\ \left[\bar{c}_m\right] & \left[\bar{d}_m\right]\end{bmatrix} = \begin{bmatrix}\left[a_m\right] & \left[b_m\right] \\ \left[c_m\right] & \left[d_m\right]\end{bmatrix}^{-1} \begin{bmatrix}\left[g_m\right] & \left[o\right] \\ \left[o\right] & \left[k_m\right]\end{bmatrix} \tag{55}$$

Substitution of equations (22), (25), and (46) into equation yields

$$[s_m^f]\{p_{xm}\} + [r_m^f]\{p_{ym}\} - \left[[h_m^f] + (h/E)[\beta_m^f]\right]\{q_m\}$$

$$-[\beta_m^f]\{W_m\} = \{0\} \tag{56}$$

Four sets of equations are now available for determining the unknown coefficients. Equations (47), (48), (56), and (37) may now be written in combined matrix form as

$$[\bar{A}_m]\begin{Bmatrix}\{p_{xm}\}\\ \{p_{ym}\}\\ \{q_m\}\\ \{W_m\}\end{Bmatrix} = [\bar{B}_m]\begin{Bmatrix}V_m\\ M_m\end{Bmatrix} \tag{57}$$

The coefficients of $\bar{A}_m$ and $\bar{B}_m$ may be identified from the four equation sets. If the series expressions, equations (20) - (25) are truncated at n = 2N, equation (57) represents 4N linear algebraic equations that must be solved for each value of m required by the series expression for the applied shears and moments given in equations (18) and (19).

Once a finite number of p_{xmn}, p_{ymn}, q_{mn}, and W_{mn} are determined from the solution to equation (57), the interface stresses may be obtained directly from equations (23) - (25). The displacements may be obtained from equations (20) - (22) in conjunction with equations (28), (44), (45), and (46).

SYMMETRIC DEFORMATION

When a stiffened panel is subject to normal pressure the flange of the stiffener and the skin are deformed symmetrically about the center line of the flange. In this case, the displacements and interface stresses may be represented in the following series form with n = 0, 2, 4, . . . ; m = 0, 1, 2, 3, . . . :

$$u = \sum_m \sum_n U_{mn} P_n (\bar{y}) \cos m\pi\bar{x} \tag{59}$$

$$v = \sum_m \sum_n V_{mn} P_{n+1} (\bar{y}) \sin m\pi\bar{x} \tag{58}$$

$$w = \sum_m \sum_n W_{mn} P_n (\bar{y}) \sin m\pi\bar{x} \tag{60}$$

$$p_x = \sum_m \sum_n p_{xmn} P_n (\bar{y}) \cos m\pi\bar{x} \tag{61}$$

$$p_y = \sum_m \sum_n p_{ymn} P_{n+1} (\bar{y}) \sin m\pi\bar{x} \tag{62}$$

$$q = \sum_m \sum_n q_{mn} P_n (\bar{y}) \sin m\pi\bar{x} \tag{63}$$

Using exactly the same procedure, all equations presented for the previous antisymmetric case are applicable if the following expressions are used instead of those defined in the previous section:

$$a_{mjn} = \bar{m}^2 A_{11} \delta_{jn}/(2n+1) + A_{66} P_j (1) P'_n (1)$$

$$b_{mjn} = \bar{m} [A_{66} P_{n+1} (1) P_j (1) - (A_{12} + A_{66}) \delta_{jn}]$$

$$c_{mjn} = -\bar{m} A_{21} P_n (1) P_{j+1} (1)$$

$$d_{mjn} = A_{22} P_{j+1} (1) P'_{n+1} (1) + \bar{m}^2 A_{66} \delta_{jn}/(2n+3) + k_y P_{n+1} (1) P_{j+1} (1)$$

$$g_{mjn} = b^2 \delta_{jn}/(2n+1)$$

$$k_{mjn} = b^2 \delta_{jn}/(2n+3)$$

$$s_{mjn} = -\bar{m} e b^3 \delta_{jn}/(2n+1)$$

$$r_{mjn} = -e b^3 P_j (1) P_{n+1} (1)$$

$$h_{mjn} = b^4 \delta_{jn}/(2n+1)$$

$$\beta_{mjn} = (\bar{m}^4 D_{11} - \bar{m}^2 b^2 N_x)\,\delta_{jn}/(2n+1)$$

$$+ P'_j(1)\,[D_{22} P''_n(1) - D_{21}\,\bar{m}^2 P_n(1)]$$

$$- P_j(1)\,[D_{22} P'''_n(1) - (D_{12}+4D_{66})\,\bar{m}^2 P'_n(1) + N_y b^2 P'_n(1)]$$

$$+ (k_z/2)\, b\, P_n(0)\, P_j(0)$$

$$Z_{mjn} = -\bar{m} A^F_{66} P'_n(1) P_j(1)$$

$$\bar{Z}_{mjn} = A^F_{22} P''_n(1) P_{j+1}(1) - \bar{m}^2 A^F_{66}\,\delta_{jn}$$

EXAMPLES

To illustrate the application of the analysis procedure described in the previous sections, the stresses at the interface of a stiffener flange and a skin plate representative of postbuckled, large cargo aircraft fuselage construction are calculated. The flange laminate is $(90/\pm45/0)_s$ and the skin laminate is $(90/\pm45/0_2/\mp45/90)_s$. Both laminates are 5 mil graphite epoxy tape. The half-wavelength, a, of the assumed buckle is 5 inches and the flange width, b, is 0.75 inch. A 0.01 inch thick adhesive serves as the interface layer. The elastic and shear moduli of the adhesive are 245,180 psi and 93,400 psi, respectively. The rapid convergence of the analysis procedure and the effects of several physical parameters on the interface stresses are demonstrated in the following examples.

CONVERGENCE

To examine the convergence properties of the analysis procedure, consider the antisymmetric case with flange and skin laminates as defined above and with the skin plate subject to a unit applied moment

$$M = (1) \sin \pi x$$

The maximum interface normal and shear stresses are plotted in Figure 3 as ratios

of computed to converged values for various numbers of terms N in the series expressions, equations (20)-(25). With N = 4, stresses are within 3 percent of the converged value. With N = 8, all stresses are within 0.1 percent of the converged value. These results apply to the condition of zero rotational restraint k_r. The presence of rotational restraint results in a reduced rate of convergence as shown in Figure 4. With $k_r = 10^3$, 12 terms are required to bring all of the stresses within 3 percent of the converged value. Similar convergence characteristics may be shown for applied shear loads and for the symmetric load cases. In all results presented in the following sections, 12 terms were used in the computations.

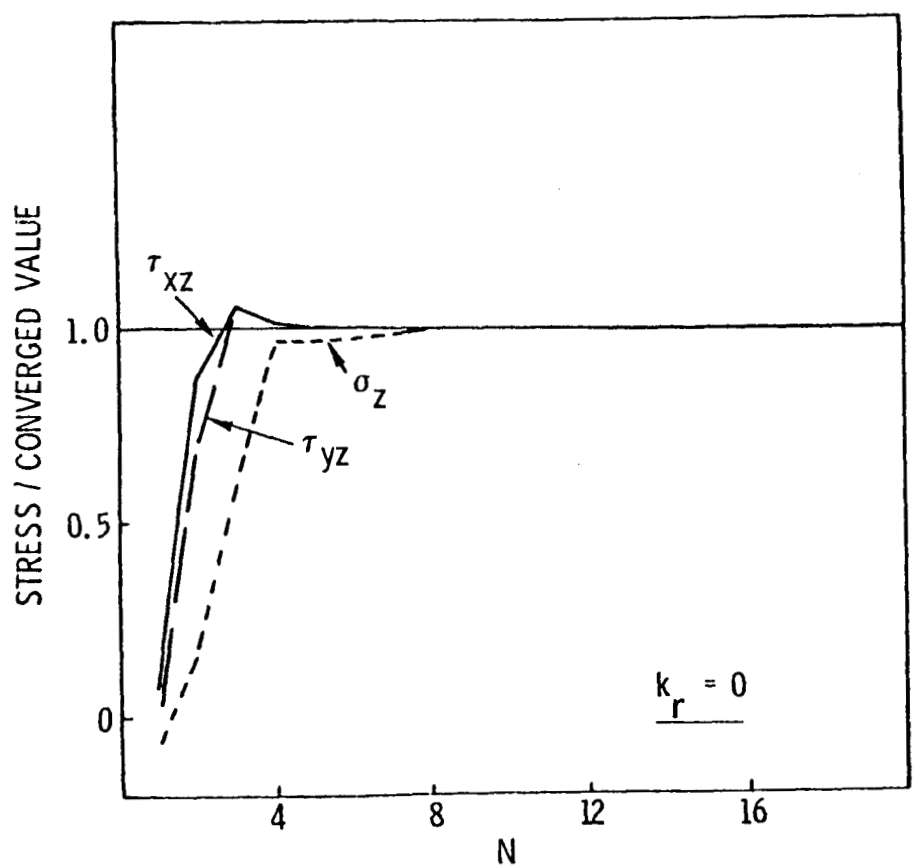

Figure 3. Convergence of Solution Procedure ($k_r = 0$)

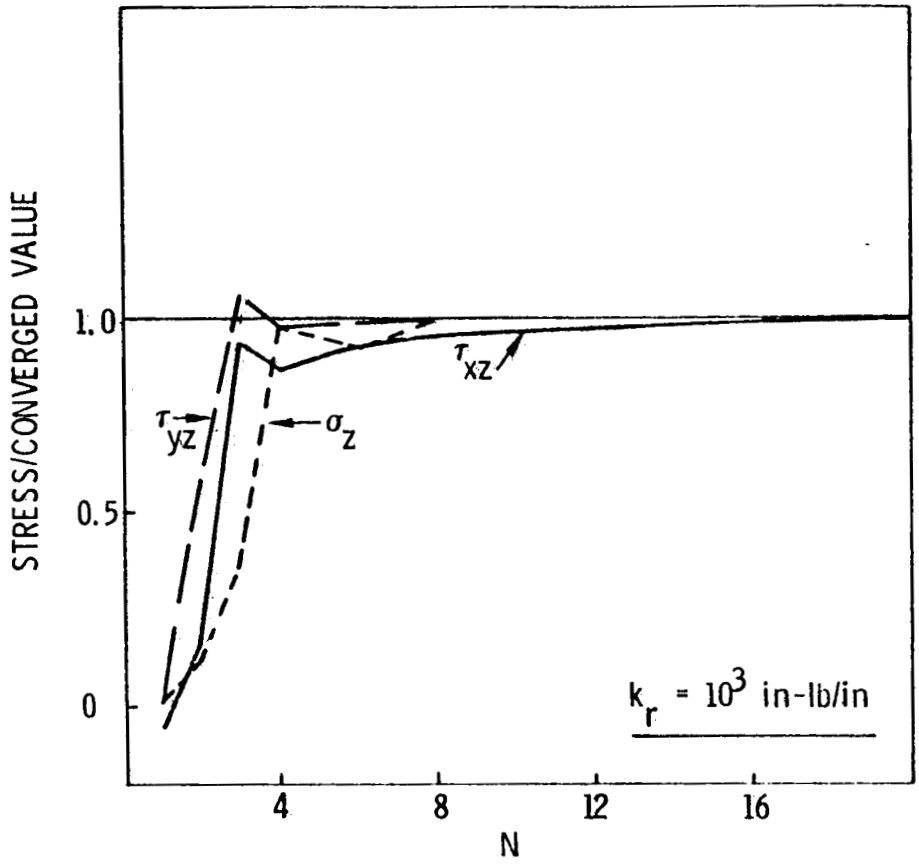

Figure 4. Convergence of Solution Procedure ($k_r = 10^3$ in-lb/in)

STRESS DISTRIBUTION

The distribution of the interface stresses across the flange width is shown in Figure 5 for the antisymmetric case with $k_r = 0$ and a unit applied moment. The stresses shown are the maximum values that occur over the length "a". The localized distribution of normal stress and the more uniform distribution of the shear stresses is typical for cases with zero elastic restraint along $y = z = 0$.

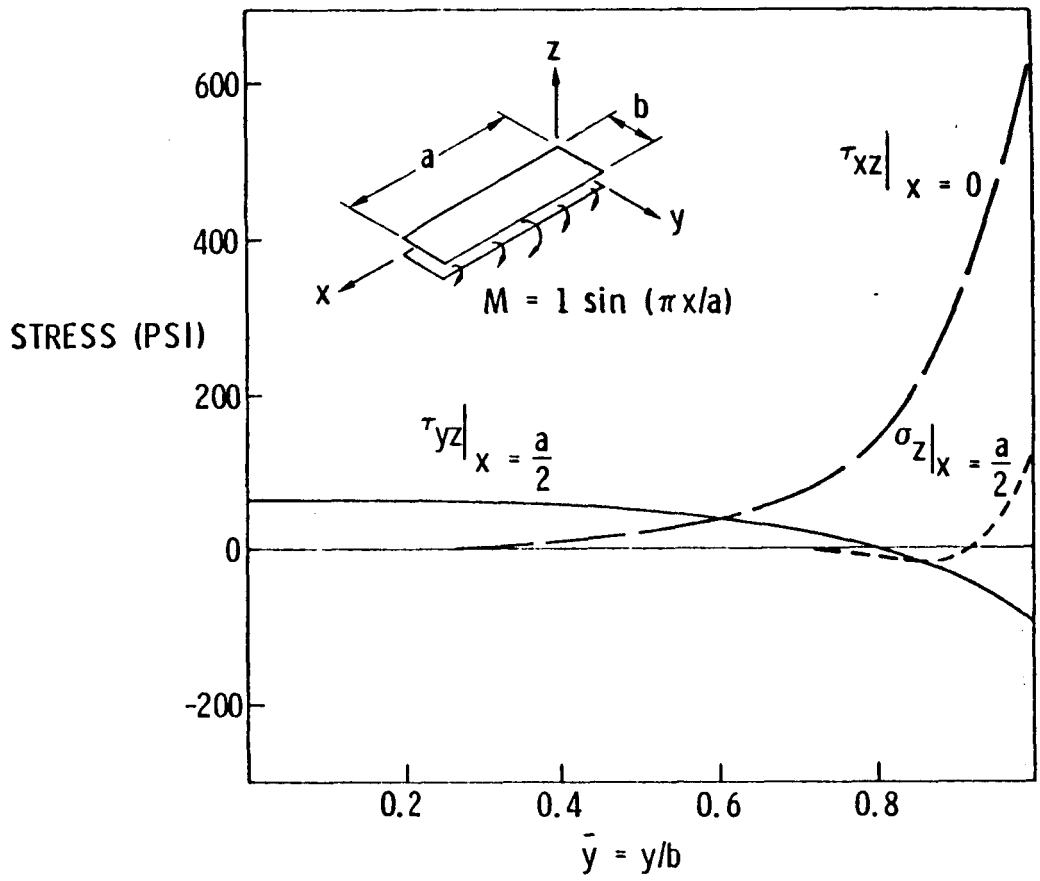

Figure 5. Interface Stress Distribution, Antisymmetric Condition

ROTATIONAL RESTRAINT

The effects that rotational restraint k_r has on the interface stresses for the case discussed above are shown in Figures 6-8. The normal stress (Figure 6) at the flange edge is essentially unaffected by the rotational restraint. A large normal stress, however, results near the restraint due to the restraining moment acting on the flange plate. If the restraint is large in magnitude, this normal stress may exceed the normal stress at the flange edge. Similar effects of rotational restraint on the shear stress, τ_{yz}, may be seen in Figure 7. The effects of rotational restraint on the shear stress, τ_{xz}, are, to the contrary, strictly beneficial as shown in Figure 8.

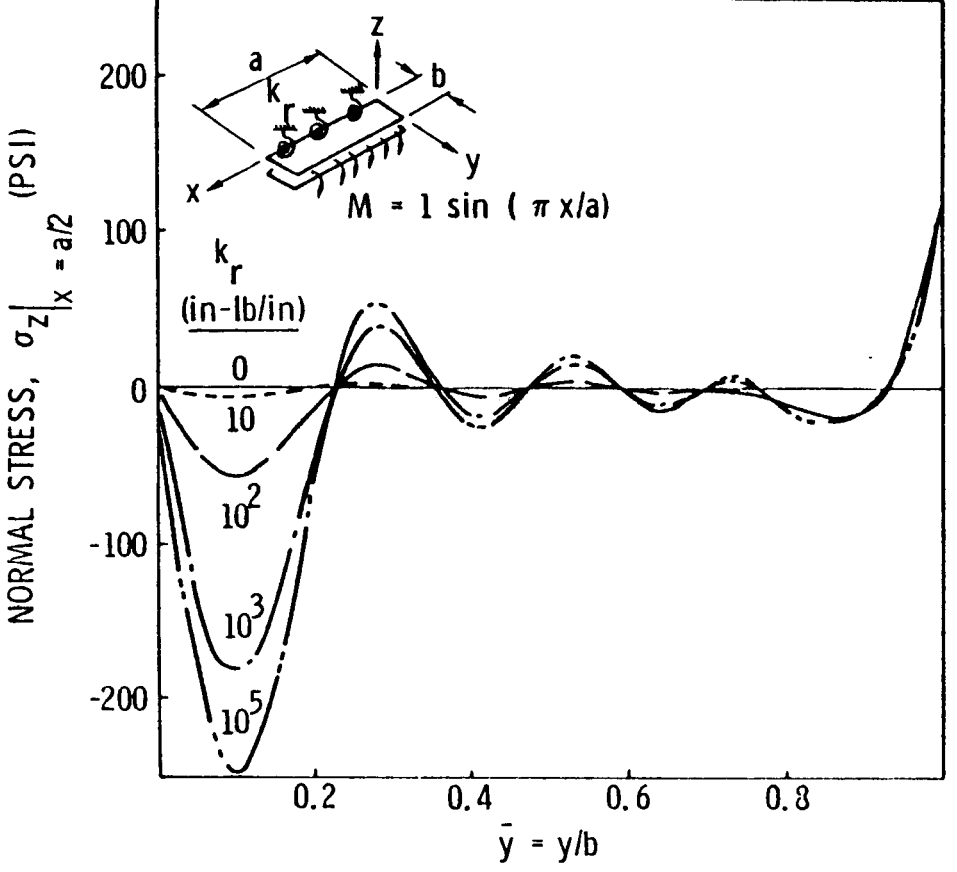

Figure 6. Effect of Rotational Restraint on Normal Stress

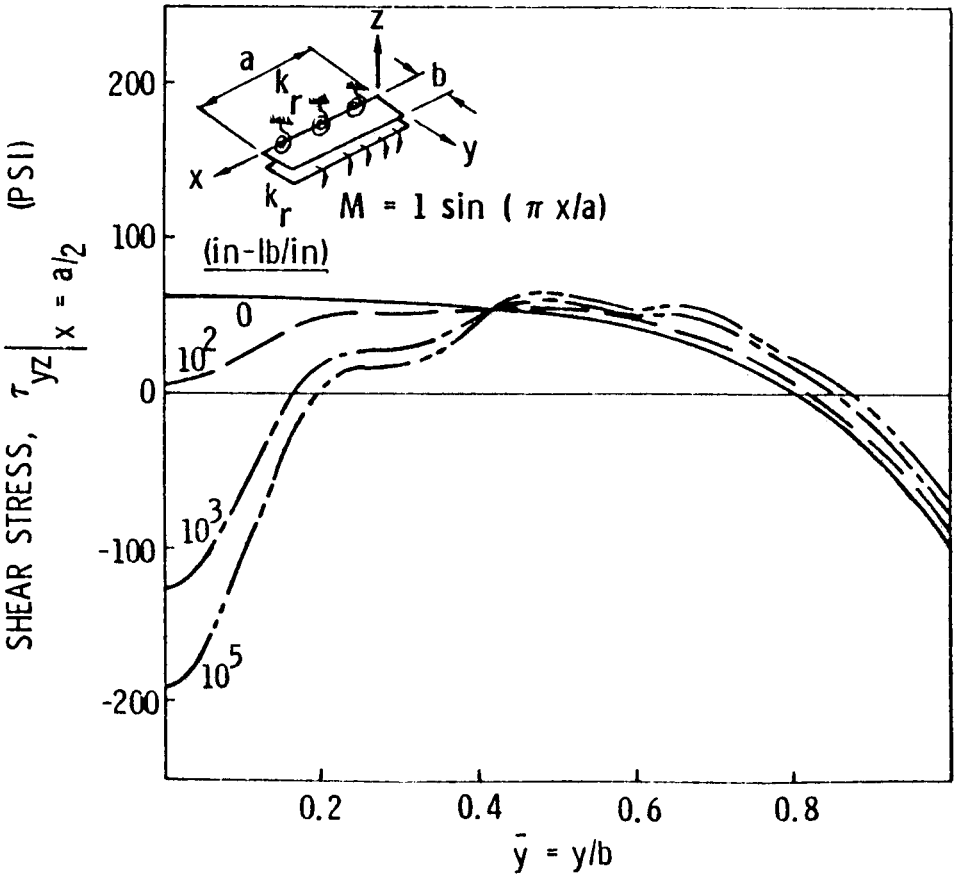

Figure 7. Effect of Rotational Restraint on Shear Stress, τ_{yz}

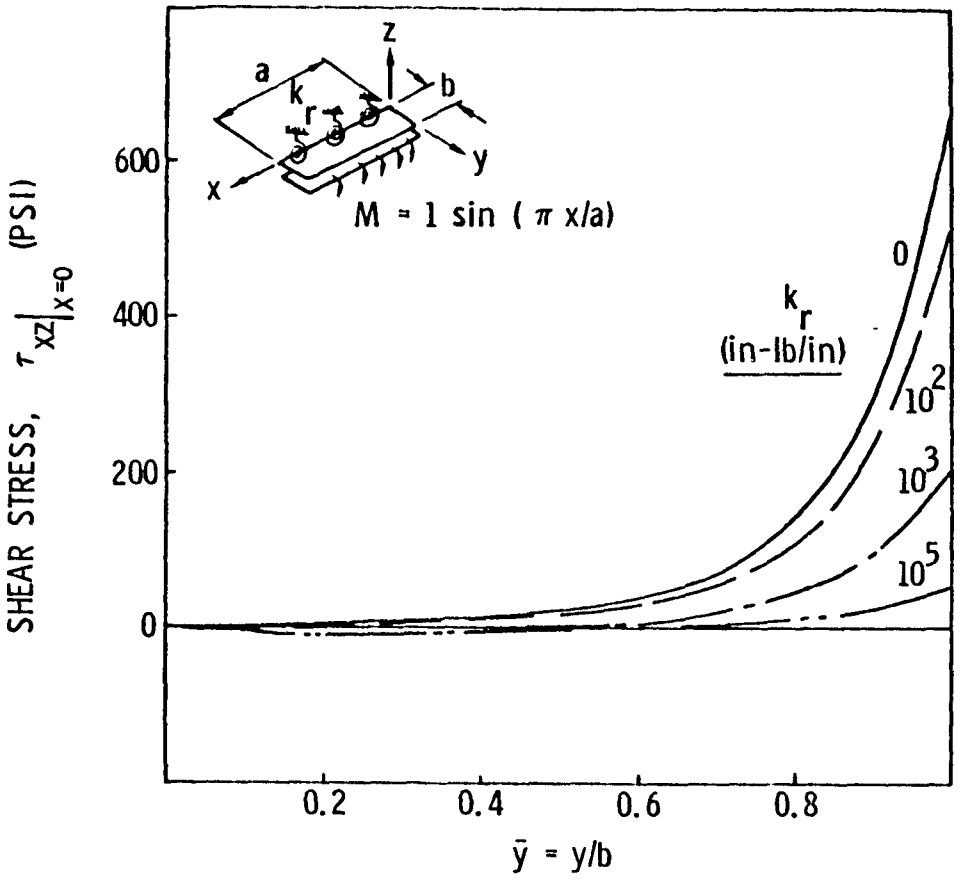

Figure 8. Effect of Rotational Restraint on Shear Stress, τ_{xz}

The strong effect of rotational restraint on the interface stresses is evident from these results. Clearly an intermediate value of restraint should be provided to minimize both normal and shear stresses. Since this restraint is primarily a function of the bending stiffness of the stiffener web plate in the short direction and the torsional properties of the stiffener, an optimum value may be provided by specifying an appropriate web laminate and stiffener geometry. Due to their low torsional stiffness blade stiffeners may not provide sufficient rotational restraint.

AXIAL COMPRESSIVE LOAD

The axial compressive load in a stiffened panel directly affects the extent of postbuckling in the panel and, therefore, the magnitude of the shear V $(\bar{x})$ and moment M $(\bar{x})$ treated as applied loads in this analysis procedure. Aside from this effect, the compressive loads in the flange and skin under the flange increase the interface stresses due to the destabilizing effect of the compressive loads.

Partial verification of the analysis procedure may be obtained by studying the effects of axial compressive loads on the interface stresses. Figure 9 shows the results of such a study. If the interface moduli are reduced to essentially zero, the flange and skin plate become uncoupled. The solid lines in this figure represent this condition. The normal stress diverges at two values of load in the skin, N_x, indicating two unstable conditions. These two values of load correspond exactly to the buckling loads of the independent flange ($N_x^f = 0.5\ N_x = 282$ lb/in) and skin ($N_x = 2590$ lb/in) plates. With a realistic interface elastic modulus E and an essentially zero shear modulus G, the results shown by the short-dashed lines are obtained. In this case, the partially coupled plates have a single buckling load between the independent buckling loads. Here the flange tries to buckle at a low load but is restrained by the skin plate through the interface normal stresses. The load can be increased until the destabilizing effect of the flange overcomes the resistance of the skin and the two-plate system buckles. If an interface with realistic E and G is used, buckling occurs at a load higher than either independent plate buckling load. As E and G increase (not shown) the buckling load approaches that of a single laminate defined by flange/interface/skin laminates. Additional effects of compressive load are shown in the following section.

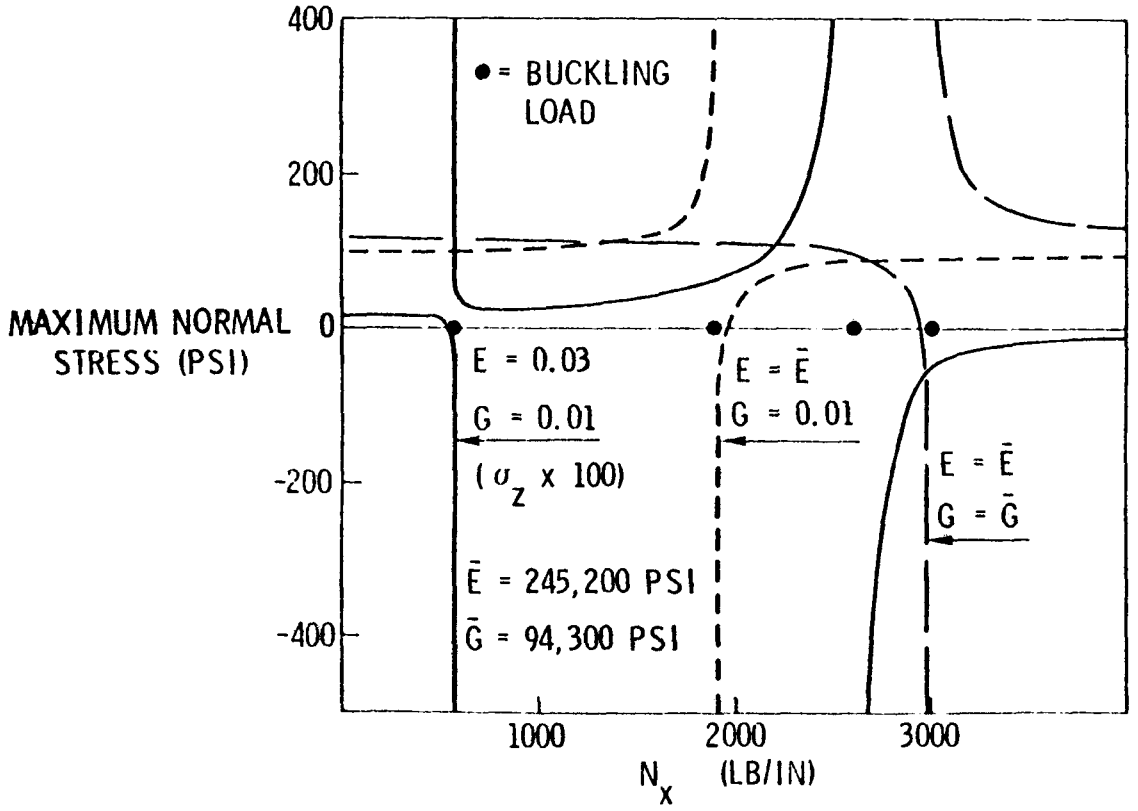

Figure 9. Buckling Loads for Coupled and Uncoupled Plates

FLANGE WIDTH

The width of the attached flange of the stiffener is an important design parameter. Interface stresses for the previously defined example case are shown in Figures 10 and 11 as functions of flange width b. Figure 10 represents the case in which the rotational restraint k_r is zero. The maximum normal stress and shear stress τ_{yz} are not strongly affected by an increase in b unless significant compressive load N_x is present and an instability condition is approached. On the other hand, the maximum shear stress τ_{xz} increases rapidly as b increases even with $N_x = 0$. Compressive load simply amplifies the increase in τ_{xz} with increasing flange width. Similar results are shown in Figure 11 for the case with $k_r = 10^3$ lb-in/in. The trends here are similar in most respects to the previous case ($k_r = 0$) but are somewhat less dramatic. The results of both cases demonstrate the benefit of a narrow attached flange.

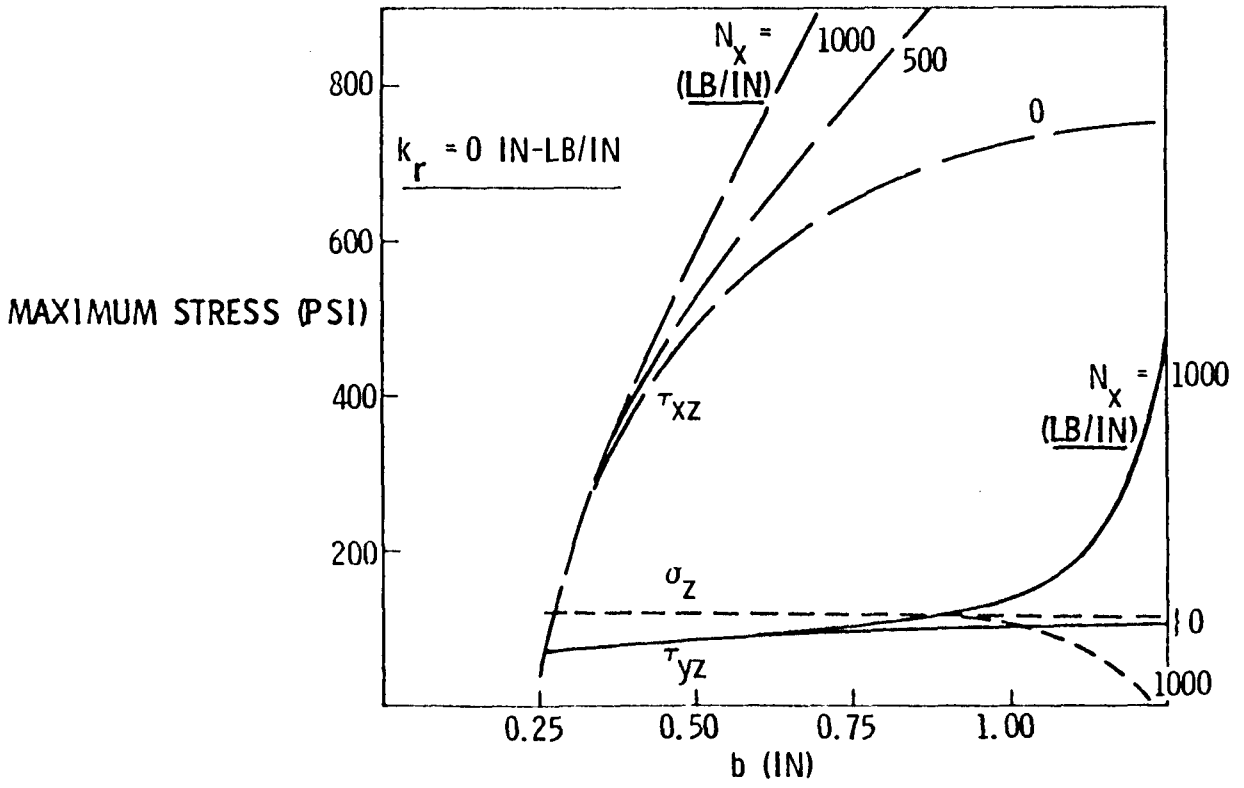

Figure 10. Effect of Flange Width and Axial Load on Maximum Stresses ($k_r = 0$)

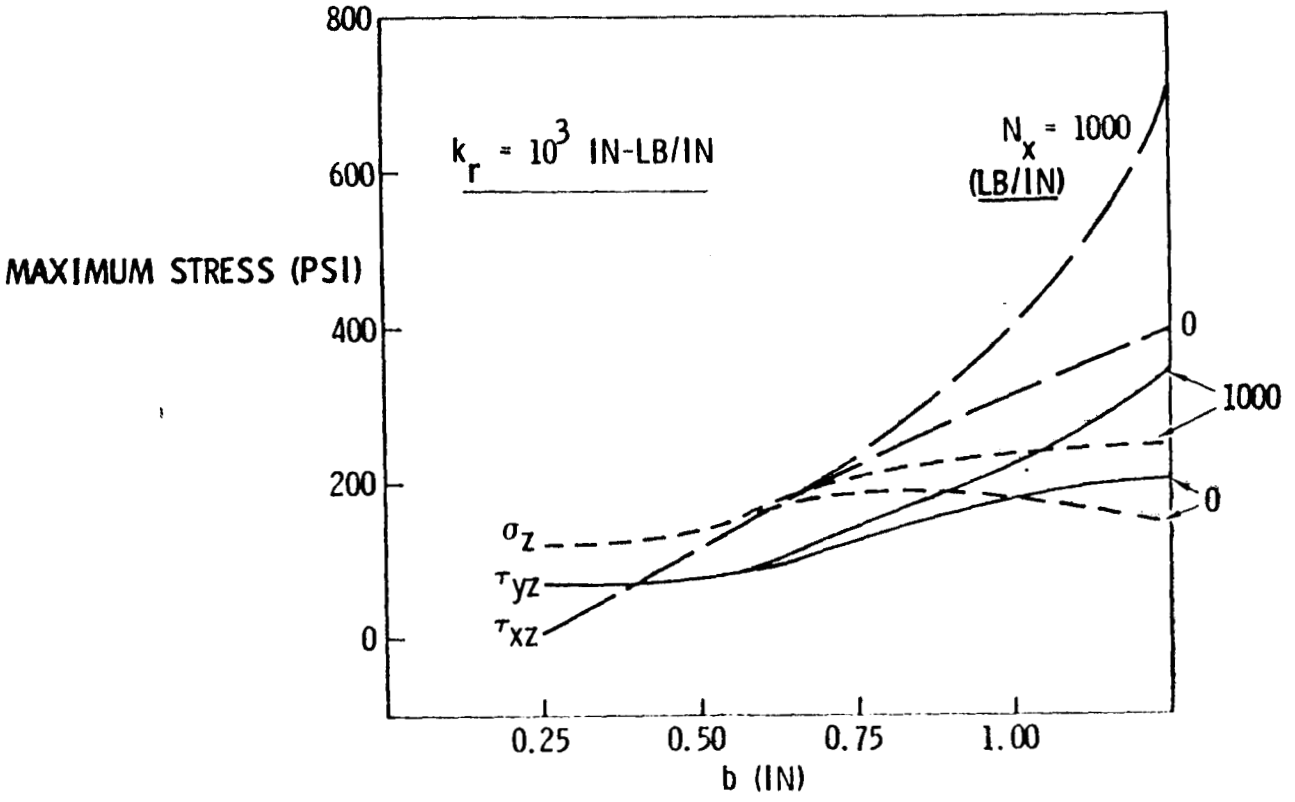

Figure 11. Effect of Flange Width and Axial Load on Maximum Stresses ($k_r = 10^3$ in-lb/in)

RELATIVE THICKNESS

The relative thickness and resulting relative bending stiffnesses of the flange and skin plates have a significant effect on the interface stresses. Since the skin laminate may be locally thickened under the flange with the addition of a pad or strap, and since the flange thickness is not strongly constrained by strength or stability requirements, the relative flange to skin thickness becomes an important and adaptable design variable.

Consider the same case as in the previous examples but only with rotational restraint $k_r = 10^3$ in-lb/in. Normal stresses for five combinations of different flange and skin laminate thicknesses are shown in Figure 12. The previously defined baseline flange and skin laminates are denoted F1 and S1, respectively. Thicker flange and skin laminates are denoted by F2, F3 and S2. Cases (F1, S1), (F2, S1) and (F3, S1) show that as the flange thickness is increased with no change in the skin, the peak normal stress decreases near $\bar{y} = 0.1$ but increases

at $\bar{y} = 1.0$. The same trend is evident when cases (F1, S2) and (F2, S2) are compared. On the other hand, as the skin thickness is increased with no change in the flange, the peak normal stress decreases significantly at both $\bar{y} = 0.1$ and $\bar{y} = 1.0$. This can be verified by comparing cases (F1, S1) and (F1, S2) as well as cases (F2, S1) and (F2, S2).

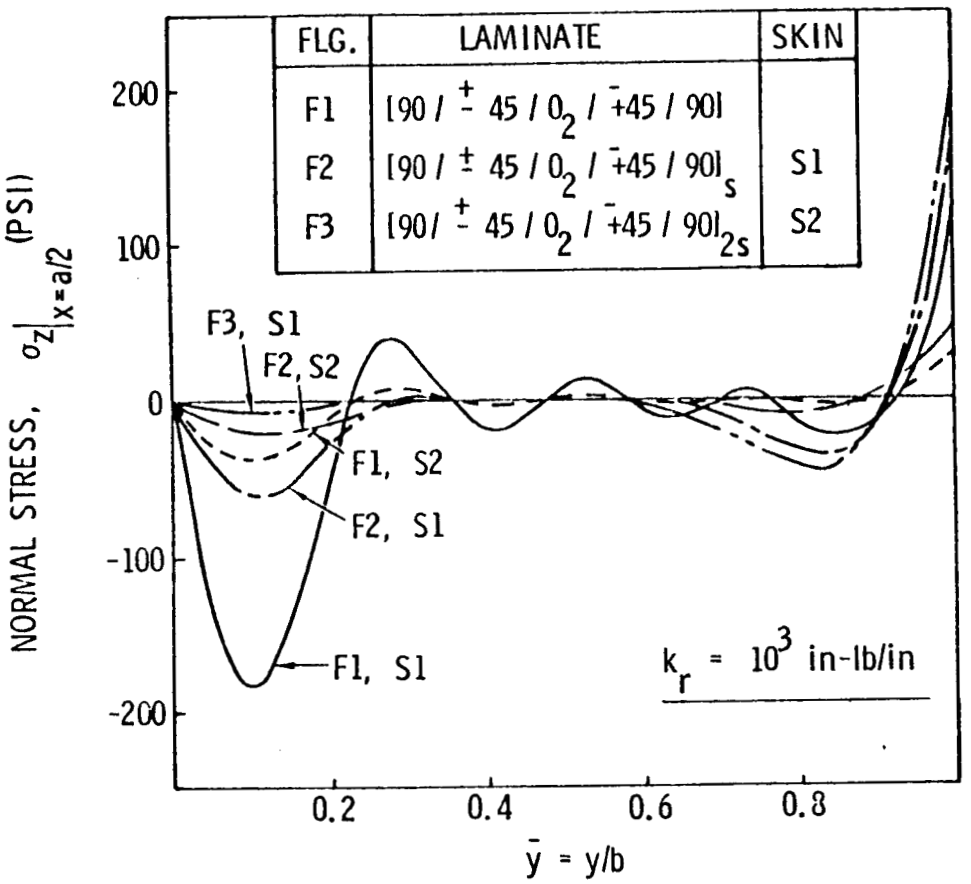

Figure 12. Effect of Relative Thickness of Plates on Normal Stress

The effects of relative thickness on interface shear stresses are essentially identical to those discussed above for normal stress. Similar results can also be shown for the symmetric load condition.

LAMINATE STACKING SEQUENCE

The stacking sequence used in laminated plates affects the bending stiffnesses D_{ij}. Therefore, just as the laminate thicknesses have significant effects on interface stresses, the stacking sequences may also have sizable effects on these stresses. As an example, consider the three flange laminates listed in Figure 13. The first laminate, the baseline used in the previous examples, appears to be the best of the three in this case. Simply interchanging the 0 and 90 degree plies results in a 42 percent increase in maximum normal stress and smaller increases in shear stresses. This shows that careful attention must be paid to the laminate stacking sequences.

FLANGE LAMINATE	MAXIMUM STRESS (PSI)		
	τ_{xz}	τ_{yz}	σ_z
$[90/\pm 45/0]_s$	210	125	184
$[0/\pm 45/90]_s$	214	156	261
$[\pm 45/0/90]_s$	207	143	232

Figure 13. Effect of Flange Stacking Sequence on Maximum Stresses

CONCLUDING REMARKS

The examples discussed in the previous sections illustrate that much may be done to minimize the skin/stiffener interface stresses by using proper design practices in the interface region. Guidelines for designing to minimize the tendency for skin/stiffener separation are summarized below.

1. The transverse bending stiffness of the stiffener web and the torsional stiffness of the stiffener should provide significant rotational restraint. The stacking sequence of the stiffener web may be adjusted to provide the proper amount of restraint. The optimum amount of restraint will be a function of the other design parameters such as flange width, flange and skin laminate thicknesses and stacking sequences.

2. To minimize the maximum value of the shear stress τ_{xz}, the minimum practical flange width should be used. Flange width does not strongly affect the normal stress or the shear stress τ_{yz}.

3. To minimize the interface stresses at the flange edge, a thin flange and/or thick skin should be used. To minimize the stresses near the stiffener web, a thick flange and/or a thick skin should be used. Since a thick skin is desirable in both cases, a local pad in the skin under the stiffener may be considered.

4. The stacking sequences of the flange and skin laminates affect the interface stresses and may be defined to minimize the interface stresses.

REFERENCES

1. Dickson, John N. and Sherrill B. Biggers, "POSTOP" Postbuckled Open-Stiffener Optimum Panels - Theory and Capability." NASA CR-172259, January 1984.

2. Biggers, Sherrill B. and John N. Dickson, "POSTOP: Postbuckled Open-Stiffener Optimum Panels - User's Manual." NASA CR-172260, January 1984.

1. Report No.	2. Government Accession No.	3. Recipient's Catalog No.
NASA CR-172261		

4. Title and Subtitle	5. Report Date
SKIN/STIFFENER INTERFACE STRESSES IN COMPOSITE STIFFENED PANELS	January 1984
	6. Performing Organization Code
7. Author(s)	8. Performing Organization Report No.
J. T. S. Wang and S. B. Biggers	
	10. Work Unit No.
9. Performing Organization Name and Address Lockheed-Georgia Company 86 South Cobb Dr. Marietta, GA 30067	11. Contract or Grant No. NASA1-15949
	13. Type of Report and Period Covered Contractor Report
12. Sponsoring Agency Name and Address National Aeronautics and Space Administration Washington, DC 20546	14. Sponsoring Agency Code

15. Supplementary Notes

Langley Technical Monitor: Dr. James H. Starnes

16. Abstract

Panels stiffened with attached stiffeners are frequently used in aerospace, naval, and various civil engineering structures when structural weight is an important concern. If the panel is loaded so that the skin (web) enters the postbuckling regime and/or the panel is subject to normal pressure loads, the skin and stiffener tend to separate. Separation of the skin and stiffener normally indicates or participates in failure of the panel. The purpose of this study is to develop a model and solution method for determining the normal and shear stresses in the interface between the skin and the stiffener attached flange. An efficient, analytical solution procedure has been developed and incorporated in a sizing code for stiffened panels described in NASA CR-172259 and NASA CR-172260. The analysis procedure described in this report provides a means to study the effects of material and geometric design parameters on the interface stresses. These stresses include the normal stress, and the shear stresses in both the longitudinal and the transverse directions. The tendency toward skin/stiffener separation may therefore be minimized by choosing appropriate values for the design variables. The most important design variables include the relative bending stiffnesses of the skin and stiffener attached flange, the bending stiffness of the stiffener web, and the flange width. The longitudinal compressive loads in the flange and skin have significant effects on the interface stresses.

17. Key Words (Suggested by Author(s))	18. Distribution Statement
Postbuckling, Stiffened Panels, Composites, Skin/Stiffener Separation, Interface Stresses, Analysis Methods	Unclassified - Unlimited Subject Category 39

19. Security Classif. (of this report)	20. Security Classif. (of this page)	21. No. of Pages	22. Price
Unclassified	Unclassified	28	A03

For sale by the National Technical Information Service, Springfield, Virginia 22161